RESEARCH ARTICLE

[NEt₃Me][O₃], Synthesis, Crystal Growth and Crystal Structure Analysis

Jonas R. Schmid,[a] Patrick Voßnacker,[a] Martin Jansen,*[b] and Sebastian Riedel*[a]

*Dedicated to Professor Wolfgang Schnick on the Occasion of his 65ᵗʰ Birthday*

[NEt₃Me][O₃] was obtained for the first time by an ion exchange reaction in liquid ammonia. It was thoroughly characterized by X-Ray diffraction [$P2_1$; $a = 598.51(4)$ pm, $b = 1032.03(7)$ pm, $c = 723.83(6)$ pm, $\beta = 92.677(3)°$, $R = 0.0384$, 15070 reflections] applying non-spherical and spherical atomic form factors for the refinements. In contrast to previous reported ozonides, [NEt₃Me][O₃] is the first to adopt the tungsten carbide (WC) motif of cation/ anion arragemnet and shows an untypical hydrogen bond between the central oxygen atom of the ozonide and the cation. Additionally, IR spectroscopy as well as quantum-chemical calculations were applied to further characterize the compound. The obtained ozonide showed high solubility in ammonia as well as acetonitrile and good properties as a synthon in ozonide chemistry.
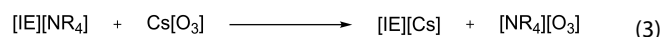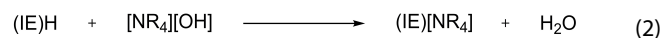
Introduction

The first observation of conspicuously colored materials forming at exposure of potassium hydroxide to ozone was already made as early as in 1868.[1] However, developing an efficient route of synthesis and unambiguously revealing the true constitution of the underlying compound as potassium ozonide, K[O₃], took more than a century. The crucial breakthrough, establishing a versatile preparative access to phase pure alkali metal ozonides, was achieved by Wolfgang Schnick as part of his doctoral thesis.[2] The procedure as developed is performed in a specific glass vessel, which allows reaction between alkali metal superoxides and gaseous mixtures of O₂/O₃ with self-regulated temperature control, extraction of the ozonide from the raw product with liquid ammonia and crystallization as high purity materials, without need to interrupt and to isolate the intermediates. Even nowadays this is still the only feasible first step in preparing ionic ozonides. Two different approaches have been optimized to realize ozonides with cations other than K, Rb, or Cs. They are based on metathesis or ion exchange, both in liquid ammonia.[3] The metathesis relies upon the usually high solubility of ozonides and the low solubility of a suitable complementary salt in liquid ammonia, as for the first time was demonstrated at the example of [NMe₄][O₃] (Equation 1).[4]

$$[NMe_4][O_2] + K[O_3] \longrightarrow [NMe_4][O_3] + K[O_2] \qquad (1)$$
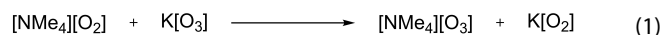
The metathesis depends on sufficiently different solubilities of the reactants. In contrast, the ion exchange route allows a more versatile exchange reaction less dependent on the solubility of the reagents. In the first step a strongly acidic ion exchange resin is charged with an alkylammonium hydroxide of choice (Equation 2). The alkali metal cation can be selectively exchanged in the second step by using an excess of the resin.[3c]

$$(IE)H + [NR_4][OH] \longrightarrow (IE)[NR_4] + H_2O \qquad (2)$$

$$[IE][NR_4] + Cs[O_3] \longrightarrow [IE][Cs] + [NR_4][O_3] \qquad (3)$$

(IE = ion exchange resin)

This box of synthesis tools has enabled to realize a large number of ionic ozonides,[3c,4] which were all characterized by single crystal X-ray diffraction. Further properties documented relate to thermal stability, magnetic susceptibility, vibrational spectroscopy and aspects of chemical bonding.[5] Although these extended studies have provided substantial insights in the chemistry and physics of ionic ozonides, some of the original objectives have not yet been attained. A long-term goal of this project has been to prepare the ground for the use of [O₃]⁻ in some follow up chemistry as a ligand, or synthon, in coordination and molecular chemistry. As a particularly attractive perspective, catenation of oxygen to chain- or ring type ions or molecules may be feasible while using the ozonide anion as a starting entity. This would include dimerization or combination with another radical cation or anion. Realization of such aims would require to have

[a] J. R. Schmid, P. Voßnacker, Prof. Dr. S. Riedel
Anorganische Chemie, Institut für Chemie Biochemie
Freie Universität Berlin
Fabeckstraße 34/36
14195 Berlin, Germany
E-mail: s.riedel@fu-berlin.de
[b] Prof. Dr. Dr. h.c. M. Jansen
Max-Planck-Institut für Festkörperforschung
Heisenbergstraße 1
70569 Stuttgart
E-mail: m.jansen@fkf.mpg.de

better soluble ozonides at hand. The only option for optimizing in this direction is to vary the cation. As another still not satisfactorily settled issue, the bond lengths and angles of the ozonide anion reported, so far, vary significantly.[5] For revealing the origin of these variations, if artifacts due to static or dynamic disorder, or consequence of intermolecular interactions via direct O—O contact or C—H···O hydrogen bonding, it appears desirable to prepare ozonides with special molecular cations that appear suited to effect some structure directing impact. Based on such motivations, in this work, we have chosen $[NEt_3Me]^+$ as a cation that might yield an ozonide with improved solubility since the conformational degrees of freedom of the ethyl substituents will enhance the entropy of dissolution for such an ozonide. Furthermore, it has been proven to be a highly stable cation towards strong oxidizers (ClF, F_2, Cl_2) and to show a tendency to form ionic liquids.[6] Additionally, the less spherical shape is expected to induce a well-ordered crystal structure.

Results and Discussion

The target compound $[NEt_3Me][O_3]$ was obtained by cation exchange from $K[O_3]$ in liquid ammonia. After removal of the potassium loaded resin and slow evaporation of ammonia, a course crystalline sample was harvested. The crystal structure was determined from single crystal X-ray data, while applying two different modes of atomic parameter refinement, the conventional one based on spherical atomic form factors (SHELX[7]) and, for localizing hydrogen atoms more accurately, with non-spherical atomic form factors (NoSpherA2 code[8]) see Table 1. The two sets of parameters as obtained are documented in Table S1.

Since the data resulting from the refinement on non-spherical atomic form factors are of better precision all respective analyses below refer to this data set. The asymmetric unit of $[NEt_3Me][O_3]$ contains only one triethyl - methylammonium ion and one ozonide anion, both are shown in Figure 1. The complex cation displays standard bond lengths and angles, c.f. Table S4.

The specific conformation of the set of ethyl ligands is apparently determined by crystal packing effects. Within realistic margins of experimental error (3 x e.s.d.) for the O—O bond lengths, the ozonide entity fulfils C_{2v} point group symmetry although no limiting crystallographic symmetry is imposed. Further, bond lengths and angle of the new ozonide fall into the range of structures of the ozonide anion as reported earlier, see Table 2.

The spread of intramolecular O—O distances from 128 to 136 pm and 113° to 120° is conspicuously large and cannot be explained by experimental deficiencies. Still, the expected tendency of changes with respect to the neutral O_3 molecule is fulfilled. Since the additional electron enters an anti-bonding MO, the O—O bonds should expand, and the O—O—O angle should narrow. Such a relation is in general met by the data available, in particular a smaller angle is associated with increased bond lengths, which corresponds to the Walsh correlation diagram relating linear and bent three atomic molecular units.[18] The substantially varying geometry of the ozonide anion appears to result from intermolecular interactions within the extended solids. Electrostatic forces as well as O···H—N or O···H—C hydrogen bonds may withdraw electron density from the ozonide thus weakening its antibonding effect. Based on this assumption, multiple interactions should decrease the antibonding character and thus shorten the bond lengths. This agrees well with experimental values when comparing the O—O bond distances of alkali metal ozonides with those of alkylammonium-based ozonides, where multiple hydrogen bonds can be found and a decrease in bond length is observed.

Several energy surface scans were performed using Orca (symmetry restraint to C_{2v} for the ozonide in the gas phase) with different functionals and basis sets to estimate the energetic feasible changes in the angle (100–130° in 1° steps) and bond length (120–140 pm in 1 pm steps) (Figure 2, Figure S5-S9, Table S5). All methods show an optimal angel close to 115° and bond length of 132 pm (MP2, SCS-MP2) or 135 pm (B3LYP D3BJ,
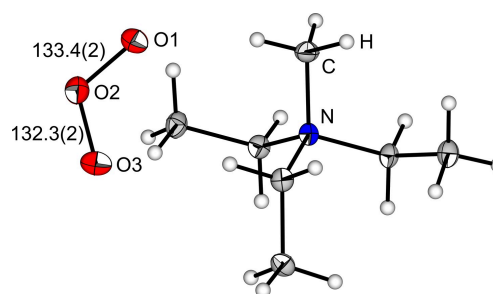
Table 1. Crystal and structure refinement data for $[NEt_3Me][O_3]$.

Sum formula	$[NEt_3Me][O_3]$
Space group, Z	$P2_1$ (No.4), 2
a/pm	598.51(4)
b/pm	1032.03(7)
c/pm	723.83(6)
β/°	92.677(3)
Volume/Å³	446.61(6)
Temperature/K	100
ρ_{calc} g/cm³	1.221
Diffractometer	Bruker D8-Venture
Radiation	MoKα ($\lambda=0.71073$)
2Θ range for data collection/°	5.64 to 56.68
Index ranges	$-7\leq h\leq 7$
	$-13\leq k\leq 12$
	$-9\leq l\leq 9$
Reflections collected	15070
Independent reflections	2164 [$R_{int}=0.0426$, $R_{sigma}=0.0300$]
Data/restraints/parameters	2164/1/173
Goodness-of-fit on F²	1.102
Final R indexes [all data]	$R_1=0.0384$ $wR_2=0.0945$
Largest diff. peak/hole / e Å⁻³	0.39/−0.18
Flack parameter	−0.5(3)

Figure 1. Crystal structure of $[NEt_3Me][O_3]$. Thermal ellipsoids set at 50% probability. Bond length O1—O2 133.4(2) pm, O2—O3 132.3(2) pm.

Table 2. Experimentally determined dimensions of the ozonide anion (crystal structures without structural disorder and refinements with $R_1 < 0.05$).

Ozonide	R(OO)/pm	⊀(OOO)/°	reference
Na[O$_3$]	135.3(3)	113.0(2)	[9]
K[O$_3$]	134.6(2)	113.5(1)	[2b, 2c]
α-Rb[O$_3$]$^{a)}$	132.9(13), 144.0(13)	108.2(17)	[10]
β-Rb[O$_3$]	134.1(6), 134.4(7)	113.7(5)	[11]
α-Cs[O$_3$]	133.3(9), 133.2(8)	114.6(6)	[12]
Cs$_3$[O$_3$]$_2$[O$_2$]·NH$_3$	132.6(4), 130.7(4)	118.7(3)	[13]
[Cs$_2$Ba][O$_3$]·2 NH$_3$	133.7(3), 135.6(3)	114.2(2)	[14]
[N(CH$_3$)$_4$][O$_3$]	128.8(3)	119.6(4)	[4a]
[N(CH$_3$)$_3$CH$_2$C$_6$H$_5$][O$_3$]	128(1), 128.2(9), 128.2(9), 127.6(9)	118.9(7), 120.4(6)	[3c]
[N(CH$_3$)$_3$C$_6$H$_5$][O$_3$]	132.1(2), 130.8(2)	117.0(2)	[3c]
[N(C$_8$H$_{16}$)$_4$][O$_3$]·1.5 NH$_3$	131.5(10), 131.7(11)	114.4(4)	[15]
[(H$_3$C)$_3$N(CH$_2$)$_6$N(CH$_3$)](O$_3$)$_2$	132.8(2), 131.9(2)	115.8(1)	[4b]
[(H$_3$C)$_3$N(CH$_2$)$_3$N(CH$_3$)$_3$](O$_3$)$_2$·3 NH$_3$	130.6(4), 130.9(4), 137.4(3), 129.5(3)	117.9(2), 114.7(2)	[4b]
[NEt$_3$Me][O$_3$]	133.4(2), 132.3(2)	116.7(1)	This work
solid ozone	127.2(0)	116.9(0)	[16]
O$_3^-$ calc.	136.1	115.4	[17]

a) The pronounced difference in the O—O bond lengths for α-RbO$_3$ results from presence of a strong intermolecular O—O interaction.[10]
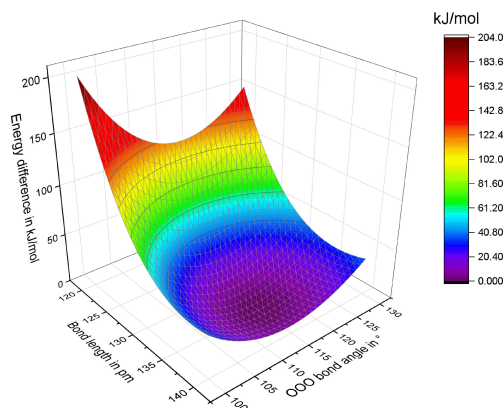
CCSD(T)), c.f. Table S5. Their local minima are in good agreement with literature values.[19]

The surface scans indicate that a change in the bond length by ±4 pm and a change in the angel by ±5° is in reasonable energetic regime (ca. 20 kJ/mol). These results agree well with previous experimentally reported angles and bond lengths (Table 2) as well as previous quantum-chemical data.[20]

By analyzing the Hirsheld surface[21] of [NEt$_3$Me][O$_3$] multiple cation anion interactions could be shown via hydrogen bonding, see Figure 3. The main interactions are between the terminal oxygen atoms and the cation and are ranging from 234(2) to 256(2) pm. Additionally, a weak interaction between the central oxygen atom and the cation (R(O2–H7A) = 254(2) pm, R(O2–C7) = 353.3(2) pm) can be identified. The O···H–C angle in the solid state structure of [NEt$_3$Me][O$_3$] is 161.1(18)°, and comes relatively close to the optimal 180° for a hydrogen bond, in contrast to 132(1)° as reported for [Me$_3$N(CH$_2$)$_3$NMe$_3$][O$_3$]$_2$).[4b] These interactions are suspected to decrease the electron density in the ozonide and therefore to weaken its anti-bonding effect, resulting in a shorter bond compared to the alkali metal ozonides.[4a,b]

By plotting the electrostatic potential of the ozonide anion on the iso-surface of the electron density an anisotropic distribution of potential can be observed, see Figure 4. A higher accumulation of charge is found approximately perpendicular to the bond axes at the terminal oxygen atoms in a belt like motif. This is in good agreement with the observed hydrogen-bonds in the molecular structure in the solid state.

Figure 3. Hirshfeld surface of [O$_3$]$^-$ in [NEt$_3$Me][O$_3$] with completed fragments in a 300 pm proximity and hydrogen bonds below 261 pm visualized by dotted lines. Thermal ellipsoids set at 50% probability. NoSpherA2 refinement shown.[21]
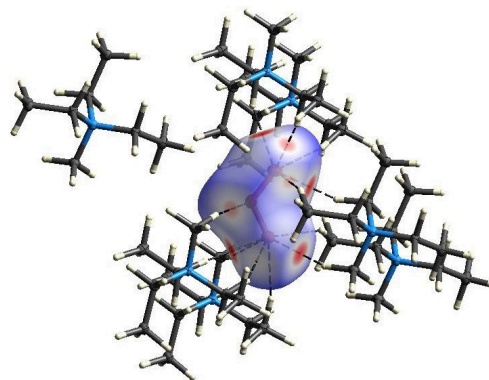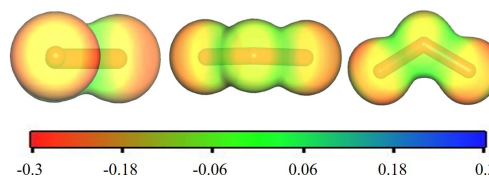

Figure 2. Energy surface scans of the ozonide along the bond angle (100–130° in 1° steps) and bond length (120–140 pm in 1 pm steps) at the CCSD(T)/def2-QZVPP level of theory (Orca) in the gas phase.

Figure 4. The electrostatic potentials of [O$_3$]$^-$ in the range of −0.3 a.u. (red) to 0.3 a.u. (blue) are mapped onto their electron densities (isosurface value 0.08 a.u.); calculated at the B3LYP-D3/def2-TZVPP level of theory (Turbomole) in the gas phase.

In contrast to most of the previously reported ionic ozonides, which adopt packing motifs corresponding to the CsCl or NaCl type of structure,[5] the building units of [NEt$_3$Me][O$_3$] arrange in a pattern according to the WC type of structure. This feature is illustrated in Figure 5 (left) and Figure S3 and S4, where the nitrogen atoms of the complex cations are connected by dashed lines. The hexagonal primitive grid as visualized offers two trigonal prismatic voids per pseudo-unit cell, half of which are occupied by an ozonide ion, thus realizing the WC motif. The space of the remaining void is filled by the alkyl side chains of the cation.
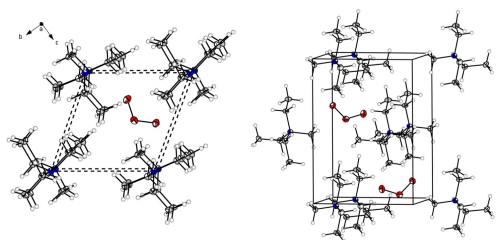

Figure 5. Perspective representation of the molecular structure in the solid state of [NEt$_3$Me][O$_3$]. Dashed lines mark the cation sphere around the anion (left) and solid lines the crystallographic unit cell (right).

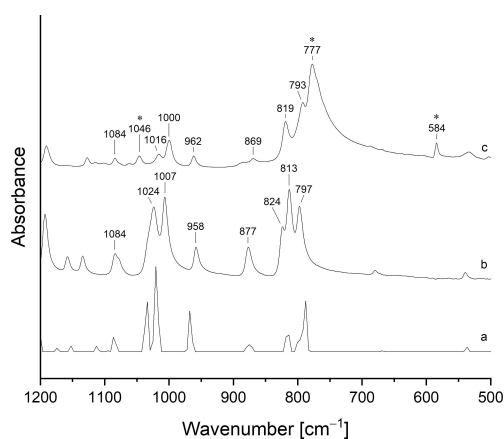**Figure 6.** Comparison of the calculated IR spectra of the cation [NEt$_3$Me]$^+$ (a, B3LYP-D3BJ/def2-QZVPP), measured spectra of [NEt$_3$Me]Cl at rt. (b) and the measured spectra of [NEt$_3$Me][O$_3$] at −70 °C (c). Ozonide specific bands are highlighted with a star.

Table 3. IR frequencies of different ozonide species in cm^{-1}.[5,9b]

[O$_3$]$^-$ calc.[a]	Na[O$_3$]	β-Rb[O$_3$]	[NMe$_4$][O$_3$]	[NEt$_3$Me][O$_3$]	Assignment referring to [O$_3$]$^-$
600	605 639	607	588	584	ν_2
883	852	800 830	782	777	ν_3
1062		1020		1046	ν_1
[a] B3LYP D3BJ/QZVPP.					

The IR spectrum of [NEt$_3$Me][O$_3$] shows three ozonide specific bands corresponding to the symmetric stretching at 1046 cm^{-1}, asymmetric stretching at 777 cm^{-1} and bending vibration at 584 cm^{-1}. These bands are in good agreement with literature values (Figure 6).[5,9b] All other bands can be assigned to the cation based on quantum-chemical calculations and a reference spectrum of the cation.

The shift in comparison to the alkali metal ozonide (Table 3), results from the mentioned interactions of the ozonide with the organic cation.

Conclusions

In summary, [NEt$_3$Me][O$_3$] could be obtained for the first time by a cation exchange reaction in liquid ammonia. Single crystals suitable for X-ray diffraction analysis were obtained from a concentrated ammonia solution, revealing an atypical WC structure type. In addition, a hydrogen bond between the cation and the central oxygen atom of the ozonide was observed, which is unusual in ozonide chemistry. Therefore, two refinements with non-spherical and spherical atomic form factors were applied to describe these interactions. The specific use of the triethylmethylammonium cation resulted in high solubilities in ammonia as well as acetonitrile and short room temperature stability, which makes it a promising synthon for upcoming ozonide chemistry. In addition, IR spectroscopy as well as an energy surface scan using various functionals and basis sets were performed to describe the new system.

Experimental Section

Synthesis of triethylmethylammonium ozonide. All water and air sensitive substances were handled under Argon (Ar 5.0) atmosphere using standard Schlenk techniques and a vacuum up to 10^{-3} mbar. If not mentioned otherwise, all syntheses were performed under stated conditions. All glassware was flame dried and joints were sealed with Triboflon grease. Ammonia (3.8 Linde) was dried by refluxed over NaK overnight, distilled and stored in a dried stainless-steel gas cylinder. The ion exchange resin Amberlyst® 15 (Merk) (2 g) was charged with triethylmethylammonium (98 %, ABCR) and was placed inside a special glass apparatus and cooled with a dry ice ethanol bath to −70 °C and the potassium ozonide[2b,c] (ca. 100 mg, 1,15 mmol) was added. Afterwards, ammonia (ca. 15 mL) was condensed onto the solids at −196 °C and the mixture was allowed to warm to −60 °C to fully dissolve the ozonide. The solution was stored at −76 °C for 3 days and extracted 3 times as described before.[3c] The red solution was concentrated under vacuum at −60 °C, transferred in a Schlenktube, concentrated again (> 1 mL) and crystallized at −76 °C.

Crystal structure determination. Single crystals were picked at −80 °C under nitrogen atmosphere and mounted on a 0.15 mm Mitegen micromount using perfluoroether oil diluted with perfluorohexane. Crystal data were collected on a Bruker D8 Venture diffractometer with a Photon 100 CMOS area detector with MoKα radiation at 100(1) K. Multiscan absorption correction was used as implemented in APEX III (SADABS-2016/2). The structures were solved with the ShelXT[7b] structure solution program using intrinsic phasing and refined with the ShelXL[7a] refinement package using least squares minimizations by using OLEX2. Hydrogen atoms were refined using HFIX 137 (CH$_3$) and HFIX 23 (CH$_2$) as implemented. Additionally, a second refinement was

carried out with NoSpherA2 (B3LYP-TZVPP, isotropic hydrogen atoms) to obtain a more accurate determination of hydrogen atom parameters.[8] Further crystallographic details are given in the supporting information. CCDC number: 2176412 (NoSpherA2), 2181389 (SHELX). For visualization the Diamond V4.65 program package was used.[22]

IR spectra were recorded on a Nicolet iS50 Advance FTIR by Thermo Fisher Scientific equipped with an ATR unit, with a Ge on KBr beamsplitter and a DLaTGS-KBr detector for MIR and a solid-substrate beamsplitter with a DLaTGS-PE detector for FIR. For low-temperature measurements a metal cylinder cooled by a cold N_2 stream was used.[16] IR (ATR, $-70\,°C$): v $= 3019$ (w), 2993 (w), 2984 (w*), 2953 (w), 1473 (m), 1451 (m), 1431 (w), 1404 (m), 1369 (w), 1358 (w), 1338 (w), 1220 (w), 1191 (m), 1127 (w), 1084 (w), 1046 (w, v_s (O_3^-)), 1016 (w), 1000 (m), 962 (w), 869 (w), 819 (m), 792 (s), 777 (vs, v_{as} (O_3^-)), 584 (m, δ (O_3^-)), 534 (w), 503 (w), 432 (w), 410 (w).*

Quantum chemical calculations were conducted using the HPC system provided by the ZEDAT (Freie Universität Berlin, Curta).[23] The programs Orca 5.0.3[24] and Turbomole 7.4.1[25] were used in combination with B3LYP,[26] MP2[27] and CCSD(T)[28] as functional and def2-TZVPP or def2-QZVPP[29] or cc-pVQZ[30] as basis set. Hirshfeld surfaces were visualized with VMD.[31]

Conflict of Interest

The authors declare no conflict of interest.

Data Availability Statement

The data that support the findings of this study are available from the corresponding author upon reasonable request.

[1] C. A. Wurtz, *Dictionnaire de chimie pure et appliquée*, Vol. II, Hachette, Paris **1868**, p. 721.

[2] a) W. Schnick, *Ph.D. Thesis*, Univ. Hannover **1986**; b) W. Schnick, M. Jansen, *Angew. Chem. Int. Ed. Engl.* **1985**, *24*, 54; c) W. Schnick, M. Jansen, *Angew. Chem.* **1985**, *97*, 48.

[3] a) W. Hesse, M. Jansen, *Angew. Chem. Int. Ed. Engl.* **1988**, *27*, 1341; b) W. Hesse, M. Jansen, *Angew. Chem.* **1988**, *100*, 1388; c) N. Korber, M. Jansen, *Chem. Ber.* **1992**, *125*, 1383.

[4] a) W. Hesse, M. Jansen, *Inorg. Chem.* **1991**, *30*, 4380; b) H. Seyeda, K. Armbruster, M. Jansen, *Chem. Ber.* **1996**, *129*, 997;

[5] c) W. Klein, M. Jansen, *Z. Naturforsch.* **2001**, *56*, 287; d) W. Assenmacher, M. Jansen, *Z. Anorg. Allg. Chem.* **1995**, *621*, 431.

[5] M. Jansen, H. Nuss, *Z. Anorg. Allg. Chem.* **2007**, *633*, 1307.

[6] a) J. R. Schmid, P. Pröhm, P. Voßnacker, G. Thiele, M. Ellwanger, S. Steinhauer, S. Riedel, *Eur. J. Inorg. Chem.* **2020**, *2020*, 4497; b) P. Voßnacker, A. Wüst, T. Keilhack, C. Müller, S. Steinhauer, H. Beckers, S. Yogendra, Y. Schiesser, R. Weber, M. Reimann, R. Müller, M. Kaupp, S. Riedel, *Sci. Adv.* **2021**, *7*, eabj5186; c) P. Pröhm, J. R. Schmid, K. Sonnenberg, P. Voßnacker, S. Steinhauer, C. J. Schattenberg, R. Müller, M. Kaupp, S. Riedel, *Angew. Chem. Int. Ed.* **2020**, *59*, 16002; d) P. Pröhm, J. R. Schmid, K. Sonnenberg, P. Voßnacker, S. Steinhauer, C. J. Schattenberg, R. Müller, M. Kaupp, S. Riedel, *Angew. Chem.* **2020**, *132*, 16136; e) T. A. Gully, P. Voßnacker, J. R. Schmid, H. Beckers, S. Riedel, *ChemistryOpen* **2021**, *10*, 255.

[7] a) G. M. Sheldrick, *Acta Crystallogr. Sect. C* **2015**, *71*, 3; b) G. M. Sheldrick, *Acta Crystallogr. Sect. A* **2015**, *71*, 3.

[8] F. Kleemiss, O. V. Dolomanov, M. Bodensteiner, N. Peyerimhoff, L. Midgley, L. J. Bourhis, A. Genoni, L. A. Malaspina, D. Jayatilaka, J. L. Spencer, F. White, B. Grundkötter-Stock, S. Steinhauer, D. Lentz, H. Puschmann, S. Grabowsky, *Chem. Sci.* **2021**, *12*, 1675.

[9] a) W. Klein, K. Armbruster, M. Jansen, *Chem. Commun.* **1998**, 707; b) W. Klein, M. Jansen, *Z. Anorg. Allg. Chem.* **2000**, *626*, 136.

[10] A. Sans, H. Nuss, S. Mohitkar, M. Jansen, *Z. Anorg. Allg. Chem.* **2017**, *643*, 357.

[11] W. Schnick, M. Jansen, *Z. Anorg. Allg. Chem.* **1986**, *532*, 37.

[12] M. Jansen, W. Assenmacher, *Z. Kristallogr.* **1991**, *194*, 315.

[13] H. Nuss, M. Jansen, *Z. Anorg. Allg. Chem.* **2012**, *638*, 501.

[14] W. Klein, M. Jansen, *Z. Anorg. Allg. Chem.* **2000**, *626*, 947.

[15] W. Klein, *Diploma Thesis*, Univ. Bonn **1995**.

[16] R. Marx, R. M. Ibberson, *Solid State Sci.* **2001**, *3*, 195.

[17] P. Borowski, B. O. Roos, S. C. Racine, T. J. Lee, S. Carter, *J. Chem. Phys.* **1995**, *103*, 266.

[18] a) R. J. Buenker, S. D. Peyerimhoff, *Chem. Rev.* **1974**, *74*, 127; b) A. D. Walsh, *J. Chem. Soc.* **1953**, 2260.

[19] W. Koch, G. Frenking, G. Steffen, D. Reinen, M. Jansen, W. Assenmacher, *J. Chem. Phys.* **1993**, *99*, 1271.

[20] H. Nuss, J. Nuss, M. Jansen, *Z. Anorg. Allg. Chem.* **2008**, *634*, 1291.

[21] P. R. Spackman, M. J. Turner, J. J. McKinnon, S. K. Wolff, D. J. Grimwood, D. Jayatilaka, M. A. Spackman, *J. Appl. Crystallogr.* **2021**, *54*, 1006.

[22] K. Brandenburg, *DIAMOND*, Crystal Impact GbR, Bonn, **2014**.

[23] L. Bennett, B. Melchers, B. Proppe, *Freie Universität Berlin*, **2020**, published online, https://doi.org/10.17169/refubium-26754.

[24] F. Neese, *WIREs Comput. Mol. Sci.* **2011**, *2*, 73.

[25] TURBOMOLE GmbH, *TURBOMOLE V7.3. a development of University of Karlsruhe and Forschungszentrum Karlsruhe GmbH*, **2018**.

[26] A. D. Becke, *Chem. Phys.* **1993**, *98*, 5648.

[27] C. Møller, M. S. Plesset, *Phys. Rev.* **1934**, *46*, 618.

[28] G. D. Purvis III, R. J. Bartlett, *J. Chem. Phys.* **1910**, *76*, (1982).

[29] F. Weigend, R. Ahlrichs, *Phys. Chem. Chem. Phys.* **2005**, *7*, 3297.

[30] T. H. Dunning, *J. Chem. Phys.* **1989**, *90*, 1007–1023.

[31] W. Humphrey, A. Dalke, K. Schulten, *J. Mol. Graphics* **1996**, *14*, 33.